

Performance Evaluation of Phase Separation Process Using High-concentration AMP Promoted by MAPA for CO₂ Capture

Akihisa MATSUI^{1*}, Naoya OGIYAMA¹, Takumi ENDO², Jun ARAKAWA², and Takao NAKAGAKI¹

¹Department of Modern Mechanical Engineering, Waseda University, 3-4-1 Okubo, Shinjuku-ku, Tokyo 160-8555, Japan

²Business Development Dept. Resources, Energy & Environment Business Area, IHI Corporation, 3-1-1 Toyosu, Koto-ku, Tokyo 135-8710, Japan

Abstract Reduction of the energy penalty and cost of CO₂ capture from concentrated gas streams using amine-based solutions can be achieved by minimizing the energy penalty in the solvent regeneration process. High concentration 2-Amino-2-methyl-1-propanol (AMP) solution precipitates as a carbonate when enough CO₂ has been absorbed. By sending the separated carbonate to the stripper, the sensible heat of regeneration can be reduced. However, previous testing using 50 weight percent AMP solution mixed with Piperazine (PZ) with solid-liquid separation showed that the CO₂ recovery rate was limited to 65% due to the lack of PZ regeneration. To improve the CO₂ recovery rate, a novel solution and injection process were developed. N-Methyl-1,3-diaminopropane (MAPA) was selected as an alternative promoter based on reaction rate testing. Various tests were employed to characterize the behaviour of the AMP/MAPA solution under CO₂ capture and recovery conditions. The injection point was relocated to avoid the inhibition of CO₂ absorption observed when CO₂ semi-lean liquid was sent to the upper portion of the absorber. The CO₂ recovery rate and the precipitation quantity were simulated using a model built in Aspen Plus®. The novel solution and injection set-up were evaluated experimentally by a bench-scale apparatus.

1 Introduction

Carbon Capture and Storage (CCS) is widely considered as a necessary technology to meet the Paris Agreement's "well below 2°C above pre-industrial levels and pursuing efforts to limit the temperature increase to 1.5°C" (UNFCCC, 2015; IPCC, 2018). For capture of CO₂ from large scale emission point sources (e.g., thermal power stations), chemical absorption is the most widely studied and mature technology. While technically proven, the chemical absorption method has the drawback of a large energy penalty owing to the regeneration of the solvents used to capture CO₂. To maintain financial viability while reducing CO₂ emissions, further process improvement and innovation are warranted. Regeneration heat is roughly divided into three sources: sensible heat, heat of vaporization, and heat of dissociation. The sensible heat is expected to be reduced via a phase separation of CO₂-rich and CO₂-lean amine. By sending only the CO₂-rich phase to stripper, the quantity of solution circulating in stripper decrease, thereby reducing the sensible heat load.

Phase separation processes commonly researched in the CCS chemical absorption field are chilled ammonia method, liquid-liquid separation method, and solid-liquid separation method. This study utilizes the solid-liquid separation method due to its higher safety and more rapid

kinetics. In the solid-liquid separation process, a high concentration amine solution is used and a precipitated solid of protonated 2-Amino-2-methyl-1-propanol (AMP) carbonate (henceforth: carbonate) is formed. Only this solid carbonate is sent to stripper (Nakagaki *et al.*, 2013).

High concentration AMP solution of $\geq 40\text{wt}\%$ results in precipitation of solid carbonate upon CO₂ absorption. The CO₂ absorption rate of AMP is slow due to steric hindrance. However, the absorption rate of AMP is accelerated by adding a small quantity of amine with a high reaction rate with CO₂ (e.g., Piperazine: PZ) as a promoter (Ying *et al.*, 2017). To confirm whether the such results remain in solid-liquid type processes, CO₂ capture and recovery tests were performed using AMP 50wt% promoted with PZ 5wt%.

Figure 1 shows the operating conditions over the process steps of the CO₂ capture and recovery test (Nakagaki *et al.*, 2015). The arrow corresponds to each unit operation ordered by ordinal numbers which indicate condition of the CO₂ loading and temperature of the circulating solution. A solvent rich in CO₂ is cooled at the bottom of the absorber column and precipitates as carbonates. A slurry of solid carbonates mixed with a small amount of liquid amine is separated by a filter-type centrifuge, the solids are dissolved by a mantle heater, and

* Corresponding author: pineforest@toki.waseda.jp

pumped to the stripper. The separated liquid phase (CO₂ semi-lean liquid) is mixed with lean liquid regenerated in the stripper and returned to the upper portion of the absorber column. In our previous study, the operating conditions and equipment setup to prevent blockage by precipitates were designed (Teranishi *et al.*, 2016) and using this setup with AMP 50wt% promoted with PZ 5wt%, the sensible heat decreased by 15–27% compared to a liquid phase process using AMP 30wt% (Ogiyama *et al.*, 2017). However, the CO₂ recovery rate was limited to 65% due to the lack of regeneration of PZ in the stripper.

This study aimed to improve the CO₂ recovery rate by searching for effective promoter of absorbent and modifying process configuration. The candidates of effective promoter were selected from amines reported in the literature which were expected to have high regeneration performance under conditions like this phase-separation process. These amines were blended with AMP and the basic characteristics of new blended amines were evaluated. As for process modifications, the injection of separated semi-lean liquid, which is usually injected into the top of the absorber, was relocated to the middle of absorber column. The rationale for this alteration was to maintain the CO₂ absorption driving force in the upper part of the column. The alteration to the regeneration heat and CO₂ recovery rate using new blended amine solutions and the new equipment set-up were empirically evaluated.

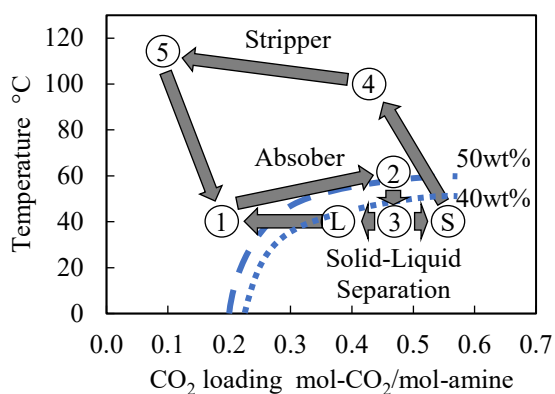


Figure 1. Process operation line of CO₂ recovery test using AMP 50wt%+PZ 5wt%. ① is the top of absorber column, ② is the bottom of absorber column, ③ is the centrifuge, ④ is the top of stripper column and ⑤ is the bottom of stripper column, L is semi-lean liquid, and S is carbonate. Two lines are boundary of precipitation in AMP 50wt% and AMP 40wt%.

2 Promoter Selection and Solution Property Evaluation

2.1 Selection of promoters based on reaction rate testing

Amines possible to react as promoter were gleaned from the literature (Bernhardsen *et al.*, 2017a, 2017b) and blended with AMP to test their performance impact.

Specifically, 1,6-Diaminohexane (HMDA), 1,4-Diaminobutane (DAB), N-(2-Aminoethyl) piperazine (AEP), Benzylamine (BZA), and N-Methyl-1,3-diaminopropane (MAPA) were evaluated. Figure 2 provides a schematic of the reaction rate test apparatus (Inoue *et al.*, 2013). A mixture of gaseous CO₂ and N₂ is supplied into the heated reactor, and the reaction rate is calculated by measuring the CO₂ concentration of the outlet gas, yielding the CO₂ absorbed per unit area. Figure 3 shows results of the testing. Although the addition of HMDA, DAB, AEP, and BZA did not accelerate the reaction rate, MAPA significantly improved the reaction rate. It has been reported that MAPA forms an eight-member ring which is easily regenerated and improves the absorption rate (Zhang *et al.*, 2018). Based on the above results, MAPA was selected as a promoter.

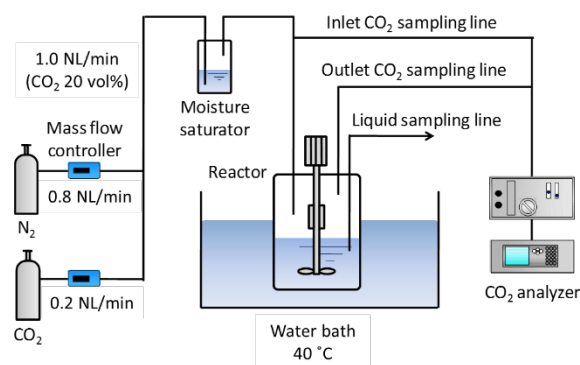


Figure 2. Static gas-liquid contactor measuring reaction rate

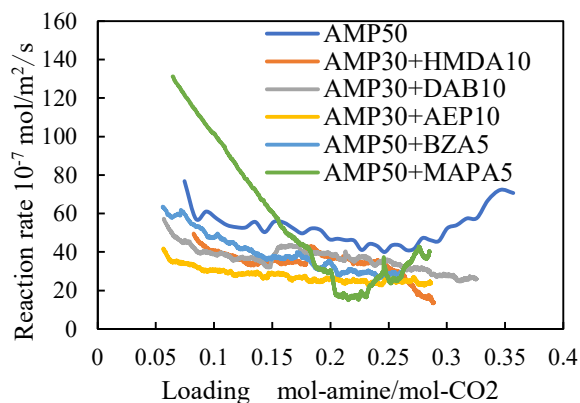


Figure 3. Results of reaction rate of various AMP-based solutions blended with promoters

2.2 Vapor-liquid equilibrium test

The vapor-liquid equilibrium characteristics of AMP 50%/MAPA 5% solution were tested in the temperature range of the absorber and stripper columns. Figure 4 shows the results of test and the results of Dash *et al.* (2011) using AMP 43wt% at 55°C. The CO₂ loading of solution was measured by the total organic carbon analyzer. From the fact that the results of Dash *et al.* (2011) fall between the 50°C and 60°C VLE plots of this test, it was concluded that the VLE behaviour of AMP was not significantly influenced by the addition of MAPA.

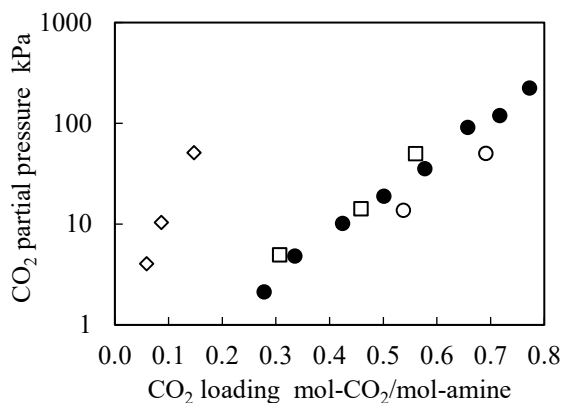


Figure 4. VLE curves of AMP 50wt%+MAPA 5wt% solution. \circ , 50°C; \square , 60°C; \diamond , 120°C; and \bullet , Dash *et al.* (2011) AMP = 43wt% at 55°C

2.3 Measurement of precipitation and dissolution temperature

Precipitation and dissolution temperature of carbonate were measured by heating and cooling solution in a glass container to determine the precipitation boundary of AMP/MAPA solution selected as described in section 2.1. CO₂ loading of solution was 0.15–0.45 (mol-CO₂/mol-amine). Figure 5 shows the measurement result and the precipitation boundary against the temperature-dependent loading. Precipitation can be avoided by maintaining a temperature >60°C under a CO₂ partial pressure of 15 kPa.

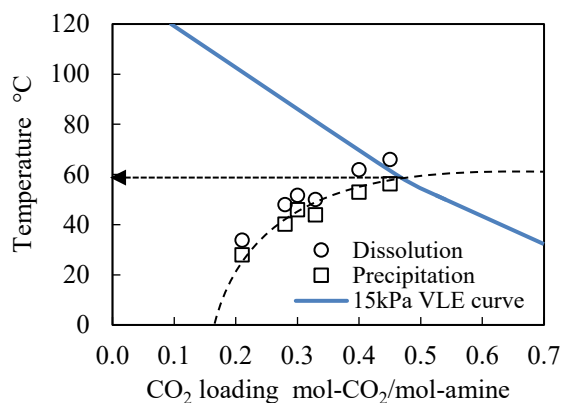


Figure 5. Boundary of precipitation against temperature and CO₂ loading. Blue line is VLE curve of CO₂ partial pressure 15kPa.

2.4 Cooling precipitation test

The cooling temperature required to induce carbonate precipitation was obtained by batch testing. The theoretical formula of Kubota (Kobari, 2014) is shown in Eq. (1), where ΔT_{ind} is the degree of supersaturation, $(N/M)_m$ is the assumed number density of primary nuclei for detection sensitivity k_{b1} is the primary nucleation constant, n is nucleation order, and ΔT is the degree of supercooling.

$$\log(\Delta T_{ind}) = \log[(N/M)_m / k_{b1}] - n \log(\Delta T) \quad (1)$$

Logarithmic plots of ΔT and lag time to precipitation are linear as shown in Eq. (1), and k_{b1} can be determined by the slope and intercept (isothermal method). After quenching 5 mL AMP 50 wt% solution, the temperature was held constant and the lag time to carbonate precipitation was measured. The primary nucleation constant was calculated from the measured time, the supersaturation degree, and the cooling temperature in the CO₂ capture and recovery test. The assumed number density of primary nuclei for detection sensitivity was set to $(N/M)_m = 500$. Figure 6 shows the results of testing, which indicates the waiting time for precipitation against the degree of supersaturation become shorter as the CO₂ loading increase. Calculating k_{b1} and n in Eq. (1) by the plots and substituting waiting time of solution in cooling container into Eq. (1) gives the required degree of supersaturation for precipitation. The CO₂ loading in the bottom of absorber was assumed to be 0.45, and the waiting time of solution in cooling container was 2010 seconds, so the degree of supersaturation was determined to be 6.4°C ($T = 53.6^\circ\text{C}$).

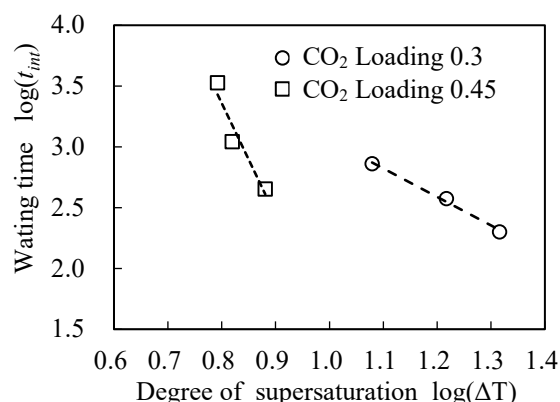


Figure 6. Waiting time for precipitation measured by isothermal method

2.5 Carbonate analysis

If MAPA is contained in the precipitates, then regeneration heat must be examined considering this MAPA-carbonate structure. Carbonate was analysed by Raman spectroscopy and gas chromatography and mass spectrometry (GC-MS) to confirm whether MAPA was contained in the precipitate. Figure 7 shows the Raman spectra of the precipitates from AMP 50 wt%, AMP 50 wt%+MAPA 5 wt%, pure AMP, and pure MAPA. Although peaks commonly observed for hydrocarbons and AMP were detected in the spectrum for AMP+MAPA, no peaks specific to MAPA were not detected (see Figure 7).

Figure 8 shows the analysis results of AMP 50 wt%+MAPA 5 wt%, AMP 100%, and MAPA 100% by GC-MS. Spectra of pure AMP and AMP 50 wt%+MAPA 5 wt% were observed at an elapsed period of 6.6 minutes, the peak of pure MAPA was observed at a period of 7.4

minutes. According to the above result, the carbonate precipitated in AMP/ MAPA solution did not contain any salts derived from MAPA.

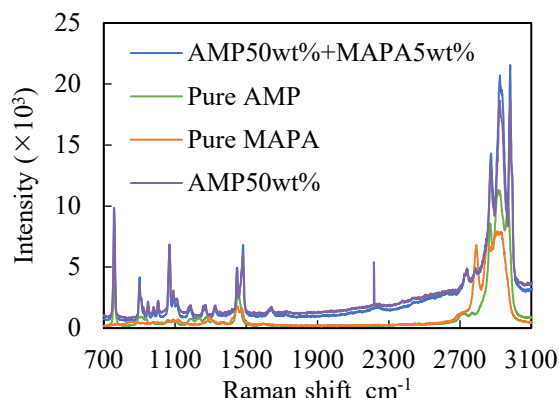


Figure 7. Raman spectra of the precipitates from the AMP 50 wt%+MAPA 5 wt%. For comparison, the spectra of pure AMP, pure MAPA, and the precipitates from AMP 50 wt% are also graphed.

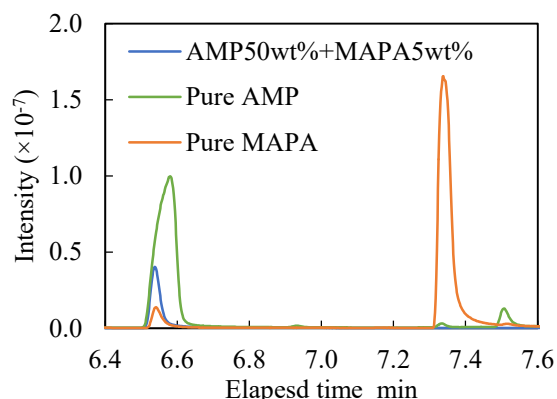


Figure 8. GC-MS spectra of precipitates from AMP 50wt%+MAPA 5wt% solution. Pure AMP and pure MAPA solution are graphed for comparison

3 Mid-column Injection Process

In our previous study of the phase separation process, separated CO₂ semi-lean liquid was mixed with CO₂ lean liquid and sent to the top of the absorber column. However, returning partially loaded solution (i.e., semi-lean liquid) to the top decreases the local absorption flux at the upper portion where is low CO₂ partial pressure. By injecting semi-lean liquid into the middle of the absorber column, the local CO₂ absorption driving force is maintained. This modification can improve the CO₂ absorption rate.

Figure 9 shows the partial model of the absorber built on the process simulator Aspen Plus[®]. The absorber column consisted of 10 stages. The change of CO₂ recovery rate and precipitate quantity was simulated when the injection stage was changed stepwise from Stage 1 (top) to Stage 10 (bottom). Figure 10 shows the calculation results of AMP 50wt% solution. The CO₂ recovery rate and the precipitate quantity peaked when semi-lean liquid was injected at Stage 5, equivalent to the

central portion of the absorber column. From this test results, the injection position of semi-lean liquid was set to the middle of the absorber column.

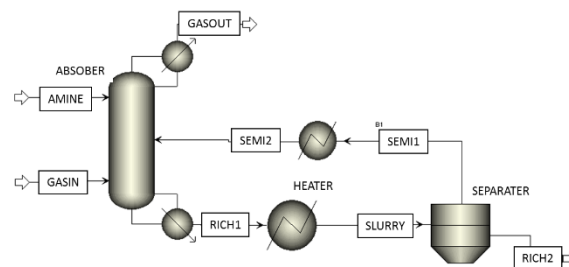


Figure 9. Partial model of absorber with variable injection location and precipitation of the CO₂-rich phase

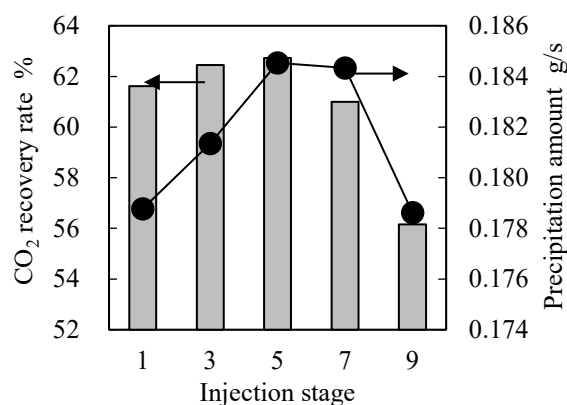


Figure 10. CO₂ recovery rate and precipitation amount at each injection stage

4 Evaluation by continuous CO₂ Capture and Recovery Test

4.1 Experimental apparatus

The new mixed amine and new injection location were evaluated by continuous CO₂ capture and recovery tests using the apparatus shown in Figure 11. The main points in the process are highlighted by numbers (1–5) and letters (S, L) in circles; these points correspond to Figure 1. The new injection location is designated by ①' in Figure 11.

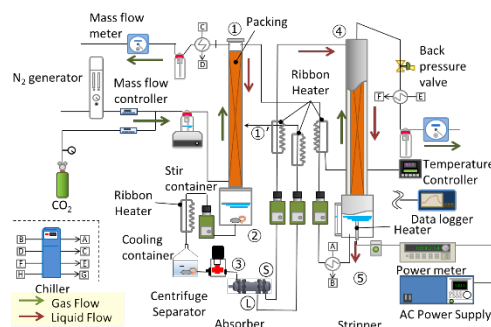


Figure 11. 10 kg/day-scale apparatus of CO₂ capture and recovery

The temperature in absorber must be maintained above the precipitation temperature to prevent passage blockage. To avoid precipitation prior to reaching the cooling container, the temperature of the lower of absorber and transfer lines to the cooling container were maintained at 65.0°C. The cooling container was chilled at the precipitation temperature of around 53.0°C by 20.0°C brine with natural cooling without insulation.

The amine concentration in solution was reduced to 40 wt% in the CO₂ capture and recovery test because the amount of precipitate increases by lowering the amine concentration under the condition of a constant liquid gas ratio.

Table 1 shows this test conditions.

Table 1. Conditions of CO₂ recovery tests using AMP 50wt%+MAPA 5 wt%

Liquid gas ratio	6
CO ₂ gas flow rate [L/min]	2.2
N ₂ gas flow rate [L/min]	12.7
CO ₂ partial pressure [kPa]	15
Upper stripper temperature [°C]	110
Lower stripper temperature [°C]	120
Electric power input of heater [W]	250

4.2 Operation stability

Operation stability of CO₂ capture and recovery test including continuous precipitation and centrifugal separation was checked by material balance of CO₂. Material balance of CO₂ can be evaluated by two way which are the CO₂ captured in the absorber, and CO₂ gas flow rate from the outlet of stripper, shown in Table 2. The difference between these flow rates was about 1.0%, and it was confirmed that the experiment was operated stably.

Table 2. CO₂ flow rate and difference between lean and rich loading of solution.

CO ₂ captured in the absorber [g/h]	217
CO ₂ gas flow rate from the outlet of stripper [g/h]	215

4.3 Regeneration heat and CO₂ recovery rate

Regeneration heat Q_{in} in this test was measured by electrical energy of the heater at the bottom of stripper compensating inherent heat loss of the stripper Q_{loss} . The CO₂ dissociation heat Q_R [GJ/ton-CO₂] was obtained by Eq. (2), where Q_V is the vaporization heat, Q_H is the sensible heat.

$$Q_R = Q_{in} - Q_V - Q_H - Q_{loss} \quad (2)$$

Q_V was obtained by Eq. (3), where the stripper vapor flow rate is given by W_V [kg/h], the latent heat is H_V [MJ/kg], and the recovery CO₂ flow rate is W_{CO_2} [kg-CO₂/h].

$$Q_V = W_V H_V / W_{CO_2} \quad (3)$$

The sensible heat was obtained by Eq. (4), where the liquid flow rate is W_S [kg/h], specific heat is C_p [MJ/kg/K], the stripper inlet temperature is T_{in} [K], and the stripper outlet temperature is T_{out} [K].

$$Q_H = W_S C_p (T_{out} - T_{in}) / W_{CO_2} \quad (4)$$

Figure 12 shows the breakdown of regeneration heat of AMP 40 wt%+MAPA 5 wt% in comparison with the previous results of AMP 50 wt%+PZ 5 wt%. The sensible heat of this test was 0.48 GJ/ton-CO₂, which corresponded to a decrease of 11–39% against the result of AMP 50 wt%+PZ 5 wt% under the same condition.

The CO₂ recovery rate was obtained by the supplied CO₂ gas flow rate and CO₂ captured in the absorber. The supplied CO₂ gas flow rate was 2.2 L/min, which corresponds to 240 g/h. Since CO₂ captured in the absorber was 217 g/h, the CO₂ recovery rate was 90%.

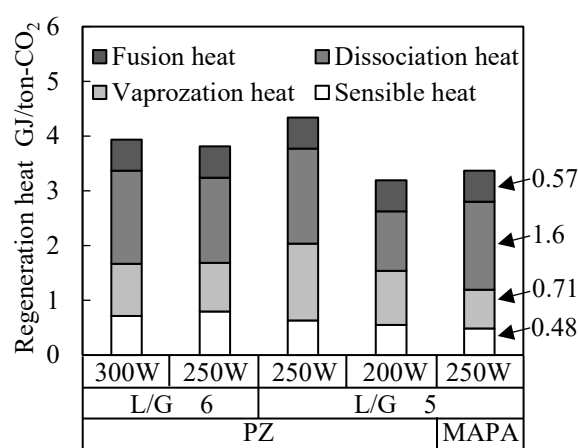


Figure 12. Regeneration heat of AMP 50wt%+PZ 5wt% and AMP 40wt%+MAPA 5wt%

5 Conclusion

This study aimed to improve the CO₂ recovery rate via selecting new promoter and modification of absorber configuration and cooling condition in the phase separation process using high-concentration AMP. The reaction rate test showed higher CO₂ absorption rate by adding MAPA than that by adding PZ, as such, AMP/MAPA solution was selected as a new solution. Simulation of the absorber column indicated that the highest CO₂ recovery rate and precipitate quantity were obtained by sending semi-lean liquid to central portion of the absorber column. In CO₂ capture and recovery tests with the new solution and the mid-column injection of semi-lean liquid, CO₂ recovery rate reached to 90% and the sensible heat was reduced to 0.48 GJ/ton-CO₂.

References

Bernhardsen, I. and H. Knuutila; "A Review of Potential Amine Solvents for CO₂ Absorption Process: Absorption

Capacity, Cyclic Capacity and pKa,” *International Journal of Greenhouse Gas Control*, **61**, 27–48 (2017a)

Bernhardsen, I., I. Krokvik, K. Jens, and H. Knuutila; “Performance of MAPA Promoted Tertiary Amine Systems for CO₂ Absorption: Influence of Alkyl Chain Length and Hydroxyl Group,” *Energy Procedia*, **114**, 1682–1688 (2017b)

Dash, S., A. Samanta, and S. Bandyopadhyay; “(Vapour + liquid) Equilibria (VLE) of CO₂ in Aqueous Solutions of 2-amino-2-methyl-1-propanol: New Data and Modelling Using eNTRL-equation,” *The Journal of Chemical Thermodynamics*, **43**, 1278–1285 (2011)

Inoue, S., T. Itakura, T. Nakagaki, T. Furukawa, H. Sato, and Y. Yamanaka; “Experimental Study on CO₂ Solubility in Aqueous Piperazine/alkanolamines Solutions at Stripper Conditions,” *Energy Procedia*, **37**, 1751–1759 (2013)

IPCC, 2018: Global Warming of 1.5°C. An IPCC Special Report on the Impacts of Global Warming of 1.5°C above Pre-industrial Levels and Related Global Greenhouse Gas Emission Pathways, in the Context of Strengthening the Global Response to the Threat of Climate Change, Sustainable Development, and Efforts To Eradicate Poverty, V. Masson-Delmotte, P. Zhai, H.-O. Pörtner, D. Roberts, J. Skea, P. R. Shukla, A. Pirani, W. Moufouma-Okia, C. Péan, R. Pidcock, S. Connors, J. B. R. Matthews, Y. Chen, X. Zhou, M. I. Gomis, E. Lonnoy, T. Maycock, M. Tignor, and T. Waterfield eds (2018) in press

Kobari, M.; “New Interpreting Crystallization Process and Solvent-mediated Polymorphic Transformation,” *JGC Technical Journal*, **6**, No.4 (2014)

Nakagaki, T., S. Inoue, S. Sato, Y. Furukawa, and H. Sato; “Evaluation of Energy in Precipitating 2-Amino-2-methyl-1-propanol Carbonate Solvent Process for CO₂ Capture,” Post-Combustion Capture Conference 2, 1a-2, Bergen, Norway (2013)

Nakagaki, T., S. Sato, H. Sato, and Y. Yamanaka; “Experimental Measurement of Regeneration Energy in CO₂ Capture System Applying Phase Separation Process using high-concentration 2-Amino-2-methyl-1-propanol,” Post-Combustion Capture Conference 3, 1B-2, Regina, Canada (2015)

Ogiyama, N., T. Hiro, H. Sato, J. Arakawa, and T. Nakagaki; “Stable Operation by Bench-scale CO₂ Capture Apparatus Applying Phase Separation Process,” The Society of Chemical Engineers, Japan 49th Autumn Meeting., CA214, Nagoya, Japan (2017)

UNFCCC, V.; “Adoption of the Paris agreement.” I: Proposal by the President (Draft Decision), United Nations Office, Geneva (Switzerland), (s 32). (2015)

Teranishi, H., H. Sato, J. Arakawa, Y. Yamanaka, and T. Nakagaki; “Modelling the Improvement of CO₂ Capture Efficiency by Way of a Novel CO₂-AMP Crystallization and Precipitation Process Using Aspen Plus,” The Society

of Chemical Engineers, Japan 48th Autumn Meeting., U121, Tokushima, Japan (2016)

Ying, J., S. Raets, and D. Eimer; “The Activator Mechanism of Piperazine in Aqueous Methyl-diethanolamine Solutions.” *Energy Procedia*, **114**, 2078–2087 (2017)

Zhang, R., X. Luo, Q. Yang, H. Yu, G. Puxty, and Z. Liang; “Analysis for the Speciation in CO₂ Loaded Aqueous MEDA and MAPA Solution Using ¹³C NMR Technology,” *International Journal of Greenhouse Gas Control*, **71**, 1–8 (2018)